

MULTIVARIABLE CONTROL DESIGN FOR INTAKE FLOW REGULATION OF A DIESEL ENGINE USING SLIDING MODE

Devesh Upadhyay*, V.I. Utkin¹ and Giorgio Rizzoni¹

* *Ford Motor Company, 1 The Ohio-State University*

Abstract: Stringent CAFÉ regulations along with technological advances in materials, high-pressure fuel injection and complex turbo charging systems have rekindled interest in the area of Diesel engines for passenger vehicle applications. A modern Diesel engine is not only clean and quiet but also allows comparable drivability relative to gasoline engines with considerable improvements in fuel economy. However the current generation diesel engine is a complex system. It is not uncommon to find features like Variable Geometry Turbo charging (VGT), Exhaust Gas Recirculation (EGR) and High Pressure Common Rail (HPCR) fuel injection. In this paper we discuss the design of a multivariable controller for the VGT-EGR system for intake flow regulation. Control design is carried out under the sliding mode framework. *Copyright © 2002 IFAC*

Keywords: Modelling, Non-linear Control, Sliding Mode, Diesel, VGT, EGR.

1. INTRODUCTION

The presence of both the VGT and EGR in the intake airflow path introduces varying degrees of complexities in the overall plant behaviour. The natural feedback established by the VGT is compromised with the presence of the high pressure EGR loop. For example an inverse response type behaviour for the compressed air flow rate in the presence of step changes in EGR position have been reported by several researchers (Kolmanovsky, et al., 1997 and Upadhyay et al., 2001). Another interesting feature that has come to light is the varying nature of the intake charge flow response to fuelling step changes under the influence of EGR (Stefanpoulou et al., 1998 Upadhyay et al., 2001). To make matters worse the diesel engine model is highly non-linear. It is no surprise therefore that the coordinated control of VGT and EGR is a difficult problem and has been so far been handled by only a few researchers (Jankovich et al., 1998 and Van Nieuwstadt et al., 2000). In (Jankovich et al., 1998) the authors use output redefinition to circumvent the nonminimum phase problem and use the domination redesign technique to design the coordinated control

with good success. In this paper we cast the VGT-EGR control problem in the sliding mode framework. We begin with a reduced order model of the plant and perform control design. The controller performance is then evaluated with respect to the full order model.

1.1 Plant model

It is possible to identify a reduced order (3state) model for the intake flow loop based on the simplifying assumptions that all thermodynamic properties are referenced to air and the intake and exhaust manifold temperature dynamics are insignificant. This approach has been adopted previously by (Utkin et al., and 2000, Jankovich et al., 1998) solely for the purpose of convenience of control design. Further modifications can be made by redefining the control inputs as the EGR flow rate and the turbine flow rate as opposed to the EGR and VGT actuator positions. The intake and exhaust pressures and the compressor power define the 3 states of the reduced order model and are as follows:

$$\dot{P}_1 = k_1 \left(\frac{\mathbf{h}_c}{C_p T_a} \frac{P_c}{\left(\left\{ \frac{P_1}{P_a} \right\}^m - 1 \right)} + W_{egr} - k_e P_1 \right) \quad (1)$$

$$\dot{P}_2 = k_2 \left(k_e P_1 + W_f - W_{egr} - W_{2t} \right) \quad (2)$$

$$\dot{P}_c = \frac{1}{\mathbf{t}_{TC}} \left(-P_c + \mathbf{h}_{im} \mathbf{h}_{is} C_p T_2 \left(1 - \left(\frac{P_a}{P_2} \right)^m \right) W_{2t} \right) \quad (3)$$

where:

$$k_1 = \frac{R_a T_1}{V_1} \quad k_2 = \frac{R_a T_{21}}{V_2} \quad k_e = \frac{\mathbf{h}_v N V_D}{R_a T_1}$$

Hence $U_1 = W_{egr}$ and $U_2 = W_{2T}$ are the two control inputs and are modelled based on standard orifice flow equations. The third input W_f is assumed to be available from a separate fuel controller. For detailed analysis of the derivations of the full order and the reduced order models the reader is referred to (Kolmanovsky et al., 1997, Upadhyay et al., 2001)

1.2 Control objectives.

The control objective is to regulate the AFR and the EGR flow fraction to the desired levels as determined from an optimised engine static calibration. These static maps are generated based on a trade-off between maximal fuel economy and minimal NO_x generation, without violating the instantaneous in time constraint on zero smoke. Hence while the set point for AFR determines the engine response and prevents smoke, the EGR flow fraction seeks to minimize in cylinder NO_x generation. If the fuelling rate is known (from driver pedal position) then the set point for AFR can be transformed into a set point for compressor flow rate W_c^d as:

$$\frac{W_c^d}{W_f} = \frac{1}{2} \left(\mathbf{b} + \sqrt{\mathbf{b}^2 + 4AFR^d(1-\mathbf{f}_g)} \right)$$

$$\text{Where } \mathbf{b} = \left(AFR^d(1-\mathbf{f}_g) + (1+AF_s)\mathbf{f}_g - 1 \right)$$

Similarly, the set point for EGR flow fraction can be expressed in terms of the desired quantities W_{egr}^d and W_c^d , as follows:

$$EGR_{ref} = \frac{W_{egr}^d}{W_c^d + W_{egr}^d} = \mathbf{f}_g$$

This allows us to transform the system outputs for regulation such that the control objective can be redefined as the regulation of the desired flow rates W_{egr}^d and W_c^d . This approach has been used previously, without details of the derivation, in (Jankovich et al., 1998, Utkin et al., 2000). Derivation details are outlined in (Upadhyay, 2001). Since real time implementation of the controller would make sense only if the controller was able to perform satisfactorily when tested on the full order model, the controller performance on the full order model was also evaluated. An obvious drawback of this approach lies in the necessity to invert the flow model to obtain the EGR valve position (\mathbf{a}) and the VGT vane position (\mathbf{b}) commands that are the control inputs to the full order model. This

inversion makes the inputs very sensitive to flow transients especially in the region where the pressure ratio across the valve approaches unity.

2. CONTROL DESIGN

As outlined in the previous section the model for the plant can be written as:

States

$$\dot{P}_1 = k_1 (W_{c1} - k_e P_1 + u_1) \quad (4)$$

$$\dot{P}_2 = k_2 (k_e P_1 - u_1 - u_2 + W_f)$$

$$\dot{P}_c = -\frac{1}{\mathbf{t}} (P_c - \mathbf{h}_m P_T)$$

Outputs as set point regulation errors

$$y_1 = W_{c1} - W_{c1}^d \quad (5)$$

$$y_2 = W_{egr} - W_{egr}^d$$

with

$$W_{c1} = \frac{\mathbf{h}_{cis} P_c}{c_p T_a} \frac{1}{\left(\left(\frac{P_1}{P_a} \right)^m - 1 \right)} \quad (6)$$

$$P_T = c_p \mathbf{h}_{is} T_2 \left(1 - \left(\frac{P_a}{P_2} \right)^m \right) u_2$$

$$u_1 = W_{egr}, u_2 = W_{2T}$$

The output regulation errors as defined in (5) are based on the definition of the control objectives. It must be pointed out that this model has a singularity at $P_1 = P_a$, however this problem can be circumvented based on the fact that it can be shown that the space $\Psi = \{(P_1, P_2, P_c) : P_1 > P_a, P_2 > P_a, P_c > 0\}$ is an invariant subspace; hence all state trajectories originating in Ψ stay in $\Psi \quad \forall t > t_0$.

3. CONTROL DESIGN WITH SLIDING MODE

A technique that is often used in sliding mode control design is the Regular Form approach. (Utkin, 1992). Unfortunately it turns out that for the model introduced in Section 1 the integrability conditions for the corresponding Pfaff system are not satisfied, hence the regular form approach cannot be easily applied to this system. It was therefore decided to use an alternate design approach in which we extend the Input-Output (IO) linearization technique to sliding mode control design.

3.1 IO Linearization for Sliding mode

We begin with an IO linearization of the VGT-EGR plant intake flow model. Recall that the output vector was defined as:

$$y_1 = W_{c1} - W_{c1}^d$$

$$y_2 = W_{egr} - W_{egr}^d$$

for this output definition following the standard IO linearization technique yields:

$$\dot{y}_1 = -\frac{(W_{c1}^d + y_1)}{\mathbf{t}} - a(W_{c1}^d + y_1 - k_e P_1) + b u_2 - a u_1$$

$$y_2 = u_1 - W_{egr}^d$$

where:

$$a = \frac{k_1 \mathbf{m} \left(\frac{P_1}{P_a} \right)^{\mathbf{m}-1}}{P_a \left(\frac{P_1}{P_a} \right)^{\mathbf{m}} - 1} W_{c1}^d; \quad b = \frac{\mathbf{h}^* T_2}{t T_a} \left(\frac{1 - \left(\frac{P_a}{P_2} \right)^{\mathbf{m}}}{\left(\frac{P_1}{P_a} \right)^{\mathbf{m}} - 1} \right)$$

$$\mathbf{h}^* = \mathbf{h}_{im} \mathbf{h}_{cis} \mathbf{h}_{is}$$

hence the vector relative degree is (1 0) and the total relative degree for the plant is 1, this implies that the internal dynamics are of the second order, note that a and b are defined in Ψ . Input-output linearization decomposes the dynamics of a non-linear system into two parts; an external (input-output) part and an internal (“unobservable”) part (Slotine et al., 1991). Stability of the internal dynamics is essential for meaningful control design. One way of analysing the internal dynamics of a system is by looking at its zero dynamics. The zero-dynamics is defined to be the internal dynamics of a system when the system output is constrained to zero by the input. It turns out that the states forming the zero dynamics can be written as:

$$\begin{aligned} \dot{P}_1 &= k_1 (W_{c1}^d - k_e P_1 + u_{1z}) \\ \dot{P}_2 &= k_2 (k_e P_1 - u_{1z} - u_{2z} + W_f^d) \end{aligned} \quad (7)$$

stability of the zero dynamics is easily established by looking at the stability of the equilibrium points. For the system in (7), the equilibrium points are:

$$\begin{aligned} P_{1e} &= \left(\frac{W_{c1}^d + W_{egr}^d}{k_e} \right) \\ P_{2e} &= \left[1 - \frac{W_{c1}^d}{W_{c1}^d + W_f^d} \frac{T_a}{\mathbf{h}^* T_2} \left(\left(\frac{P_{1e}}{P_a} \right)^{\mathbf{m}} - 1 \right) \right]^{-1/\mathbf{m}} \end{aligned} \quad (8)$$

It can be shown through a Jacobi linearization of (8) that the equilibrium is unstable and that P_{2e} is the **unstable** mode, this conclusion was also shown in Jankovich et al., (1998). Hence as stressed above control design is not meaningful for the system defined by (4) and (5). It is possible to circumvent this problem through *output redefinition*.

Consider a new set of outputs as defined below where we replace the EGR flow rate by the exhaust manifold pressure P_2 .

$$\bar{y} = \begin{bmatrix} \bar{y}_1 = W_{c1} - W_{c1}^d \\ \bar{y}_2 = P_2 - P_{2e} \end{bmatrix} \quad (9)$$

with this output definition the IO linearization yields:

$$\begin{aligned} \dot{\bar{y}}_1 &= -\frac{(W_{c1}^d + \bar{y}_1)}{t} - a(W_{c1}^d + \bar{y}_1 - k_e P_1) + b u_2 - a u_1 \\ \dot{\bar{y}}_2 &= k_2 (k_e P_1 + W_f^d) - k_2 u_1 - k_2 u_2 \end{aligned}$$

giving a vector relative degree of (1,1) and a zero dynamics of the first order. The corresponding internal dynamics for the system is represented by the state P_1 as follows:

$$\dot{P}_1 = k_1 (\bar{y}_1 + W_{c1}^d - k_e P_1 + u_1) \quad (10)$$

To establish the stability of the internal dynamics we examine the zero dynamics of the system as follows:

$$\begin{aligned} \bar{y}_1 = 0 &\Rightarrow W_{c1} = W_{c1}^d; \quad \bar{y}_2 = 0 \Rightarrow P_2 = P_{2e} \\ \dot{\bar{y}}_1 = 0 &\Rightarrow a_o (W_{c1}^d - k_e P_1) + \frac{W_{c1}^d}{t} = b_o u_{2z} - a_o u_{1z} \\ \dot{\bar{y}}_2 = 0 &\Rightarrow k_e P_1 + W_f^d = u_{1z} + u_{2z} \end{aligned}$$

hence

$$\begin{aligned} u_{1z} &= \frac{k_e P_1 (a_o + b_o) - W_{c1}^d (a_o + 1/t) + b_o W_f^d}{a_o + b_o} \\ u_{2z} &= \frac{W_{c1}^d (a_o + 1/t) + a_o W_f^d}{a_o + b_o} \end{aligned}$$

where:

$$a_o = \frac{k_1 \mathbf{m} \left(\frac{P_1}{P_a} \right)^{\mathbf{m}-1}}{P_a \left(\frac{P_1}{P_a} \right)^{\mathbf{m}} - 1} W_{c1}^d; \quad b_o = \frac{\mathbf{h}^* T_2}{t T_a} \left(\frac{1 - \left(\frac{P_a}{P_{2e}} \right)^{\mathbf{m}}}{\left(\frac{P_1}{P_a} \right)^{\mathbf{m}} - 1} \right)$$

with $\mathbf{h}^* = \mathbf{h}_{im} \mathbf{h}_{cis} \mathbf{h}_{is}$

the zero dynamics for the system is then established by substituting u_{1z} into (10) as follows:

$$\dot{P}_{1z} = \frac{k_1}{a_o + b_o} \left\{ b_o (W_{c1}^d + W_f^d) - \frac{W_{c1}^d}{t} \right\}$$

substituting the appropriate values for the variables u_{1z} ; u_{2z} ; a_o ; b_o ; P_{2e} , yields the following equation for the stable zero dynamics:

$$\dot{P}_{1z} = \frac{k_1 (W_{c1}^d + W_f^d) P_a * \left(\left(\frac{P_{1e}}{P_a} \right)^{\mathbf{m}} - \left(\frac{P_{1z}}{P_a} \right)^{\mathbf{m}} \right)}{k_1 \mathbf{m} t (W_{c1}^d + W_f^d) \left(\frac{P_{1e}}{P_a} \right)^{\mathbf{m}-1} + P_a \left(\frac{P_{1e}}{P_a} \right)^{\mathbf{m}} - P_a}$$

3.2 Extension of IO Linearization to Sliding mode

In this section we present the extension of input output linearizability to the Sliding mode technique for MIMO non-linear systems. Consider a non-linear system of the form:

$$\dot{x} = f(x) + \sum_{k=1}^m g_k(x) u_k$$

$$y_i = h_i(x); \quad i = 1..m, \quad \text{with}$$

$$u \in \mathfrak{R}^m; \quad x \in \mathfrak{R}^n; \quad y \in \mathfrak{R}^m$$

$$f, g_k, h, \quad \text{are } C^\infty \text{ vector fields on } \mathfrak{R}^n$$

we now define S as a set of surfaces $\{S_i\}$ $i = 1..m$, where each S_i can be defined as a function of the derivatives of the i^{th} output y_i upto the $(r_i - 1)^{th}$ order, where r_i is the equivalent linearizability index of the i^{th} output channel, hence,

$$S_i = \sum_{k=1}^{r_i-1} \mathbf{a}_{ik} y_i^{[k]} \quad (11)$$

where \mathbf{a}_{ik} are arbitrary coefficients to be selected by the designer and $y_i^{[k]}$ is the k^{th} derivative of y_i . It is

easy to see that if we wish to tackle a tracking problem $y_i^{[k]}$ can be replaced with $e_i^{[k]}$:

where $e_i = y_i^d - y_i$,

$$S_i = \sum_{k=1}^{r_i-1} \mathbf{a}_{ik} e_i^{[k]}$$

Working with equation (11) it can be shown that:

$$\dot{S}_i = \sum_{j=0}^{r_i} \mathbf{a}_{i,j-1} y_{id}^{[j]} - \sum_{j=0}^{r_i} \mathbf{a}_{i,j-1} L_f^j(h_i) - \mathbf{a}_{i,r_i-1} \sum_{k=1}^m L_{gk}(L_f^{r_i-1}(h_i)) u_k \quad (12)$$

for, $i = 1 \dots m$ we can write (11) in a compact form as:

$$\dot{S} = Y_d - L(x) - \mathbf{y}(x)U \quad (13)$$

where:

$$\dot{S} = [\dot{S}_1 \dots \dot{S}_m]^T$$

$$Y_d = [Y_{d1} \dots Y_{dm}]^T, \quad Y_{di} = \sum_{j=0}^{r_i} \mathbf{a}_{i,j-1} y_{di}^{[j]}$$

$$L(x) = [L_1(x) \dots L_m(x)]^T, \quad L_i(x) = \sum_{j=0}^{r_i} \mathbf{a}_{i,j-1} L_f^j(h_i)$$

$$\mathbf{y}(x) = [\mathbf{y}_1(x) \dots \mathbf{y}_m(x)]^T, \quad \mathbf{y}_i(x)U = \mathbf{a}_{i,r_i-1} \sum_{k=1}^m L_{gk}(L_f^{r_i-1}(h_i)) u_k \quad (14)$$

where, $L_f(h)$ and $L_g(L_f(h))$ are the Lie derivatives. We can now define the attractiveness condition for each surface such that

$$\dot{S}_i S_i < 0$$

a simple choice would be $\dot{S}_i = -\mathbf{I}_i \text{sign}(S_i)$, $\mathbf{I}_i > 0$, $i = 1 \dots m$, this condition can be written as:

$$\dot{S} = -M(S), \quad M(S) = [M_1 \dots M_m]^T, \quad M_i = -\mathbf{I}_i \text{sign}(S_i) \quad (15)$$

based on equation (15) it is guaranteed that sliding mode will be enforced on all surfaces $S_i = 0$, in finite time. Hence from equations (13) and (15) and assuming \mathbf{y}^{-1} exists we get:

$$U = \mathbf{y}^{-1} \{Y_d + M(S) - L(x)\} \quad (16)$$

the existence of \mathbf{y}^{-1} is a necessary condition for I/O linearization.

3.3 The VGT-EGR control design problem

Based on the discussion outlined so far we now illustrate this design process via the VGT-EGR problem at hand with the output redefinition as outlined earlier. Recall the output vector was defined as:

$$\bar{\mathbf{y}} = \begin{bmatrix} \bar{y}_1 = W_{c1} - W_{c1}^d \\ \bar{y}_2 = P_2 - P_{2e} \end{bmatrix}$$

and I/O linearization had yielded:

$$\dot{\bar{y}}_1 = -\frac{(W_{c1}^d + \bar{y}_1)}{\mathbf{t}} - a(W_{c1}^d + \bar{y}_1 - k_e P_1) + b u_2 - a u_1$$

$$\dot{\bar{y}}_2 = k_2(k_e P_1 + W_f^d) - k_2 u_1 - k_2 u_2$$

following the technique illustrated earlier we can now define the sliding surfaces as:

$$\dot{S}_1 = \dot{\bar{y}}_1 = -\frac{(W_{c1}^d + \bar{y}_1)}{\mathbf{t}} - a(W_{c1}^d + \bar{y}_1 - k_e P_1) + b u_2 - a u_1$$

$$\dot{S}_2 = \dot{\bar{y}}_2 = k_2(k_e P_1 + W_f^d) - k_2 u_1 - k_2 u_2$$

where, "a" and "b" are as defined previously and $S_i = \bar{y}_i$.

Next we define the attractiveness condition as the constant rate reaching law:

$\dot{S}_i = -\mathbf{I}_i \text{sign}(S_i)$ for $i = 1, 2$, leading to

$$-\mathbf{I}_1 \text{sign}(S_1) = -\frac{(W_{c1}^d + \bar{y}_1)}{\mathbf{t}} - a(W_{c1}^d + \bar{y}_1 - k_e P_1) + b u_2 - a u_1 \quad (17)$$

$$-\mathbf{I}_2 \text{sign}(S_2) = k_2(k_e P_1 + W_f^d) - k_2 u_1 - k_2 u_2$$

after some algebraic manipulations we get:

$$u_2 = \frac{1}{(a+b)} \left[\frac{W_{c1}(a + \frac{1}{\mathbf{t}}) + a W_f^d - \mathbf{I}_1 \text{sign}(S_1) + (a \mathbf{I}_2 / k_2) \text{sign}(S_2)}{\mathbf{t}} \right]$$

$$u_1 = \frac{1}{(a+b)} \left[\frac{-W_{c1}(a + \frac{1}{\mathbf{t}}) + (a+b)k_e P_1 + b W_f^d + \mathbf{I}_1 \text{sign}(S_1) + (b \mathbf{I}_2 / k_2) \text{sign}(S_2)}{\mathbf{t}} \right] \quad (18)$$

with the variables \mathbf{I}_i to be selected such that sliding mode is enforced in the manifold of interest.

3.4 Observer design

The controller designed relies on measurements of the intake manifold pressure P_1 , the compressor flow rate W_{c1} and the exhaust manifold pressure P_2 . The compressor power P_c can be determined from the compressed air flow rate provided the compressor efficiency \mathbf{h}_{cis} is known. Normally the exhaust manifold pressure is not available as a standard measurement hence we have to design an observer for the exhaust manifold pressure, this accomplished as follows:

Consider the compressor power state equation:

$$\dot{P}_c = -\frac{1}{\mathbf{t}} P_c + \mathbf{x} u_2 - \mathbf{x} \left(\frac{P_{amb}}{P_2} \right)^m u_2$$

where:

$$\mathbf{x} = \frac{\mathbf{h}_m \mathbf{h}_v T_2 c_p}{\mathbf{t}}$$

define observer system as:

$$\dot{\hat{P}}_c = -\frac{1}{\mathbf{t}} \hat{P}_c + \mathbf{x} u_2 - l_3 \text{sign}(\hat{P}_c - P_c)$$

the corresponding error dynamics are represented as:

$$\dot{\bar{P}}_c = -\frac{1}{\mathbf{t}} \bar{P}_c + \mathbf{x} \left(\frac{P_{amb}}{\hat{P}_2} \right) u_2 - l_3 \text{sign}(\hat{P}_c - P_c)$$

next select a sliding surface, $S = \bar{P}_c$, with $-l_3 > 0$, such that $S \rightarrow 0$ in finite time. once $S \rightarrow 0$, $\dot{S} = \dot{\bar{P}}_c = 0$

$$-l_3 \text{sign}(\bar{P}_c)_{eq} = -\frac{1}{t} \bar{P}_c - \mathbf{x} \left(\frac{P_{amb}}{\hat{P}_2} \right)^m$$

hence

$$\hat{P}_2 = \left[\frac{u_2 \mathbf{x}}{\left(\frac{1}{t} \bar{P}_c - u_{eq} \right)} \right]^{-1/m} P_{amb}$$

where u_{eq} , the equivalent control is available from a first order filter with time constant t_f as shown:

$$\dot{u}_{eq} = -\frac{1}{t_f} u_{eq} + \frac{1}{t_f} (-l_3 \text{sign}(\bar{P}_c))$$

4. SIMULATION RESULTS

During the course of this work several facts came to light after careful observation.

1. The flow through the EGR valve is dictated by the pressure ratio P_1/P_2 over the valve, as should be obvious from the standard orifice flow model.
2. The intake manifold pressure P_1 dynamics are slower than those of the exhaust manifold pressure P_2 , due to TC influence (turbolag).
3. An open EGR valve couples the dynamics of the intake and exhaust manifold pressures.

Therefore it came as no surprise that regulation of the EGR flow rate to desired flow rates was in general a more difficult task. A conclusion was reached that for satisfactory regulation of the EGR flow rate it was essential to monitor the behaviour of the pressure ratio, a smooth trajectory being desirable. Figure 1 shows the desired flow profiles for the EGR flow rate and the compressed air flow rate that was to be achieved via the coordinated control of EGR and VGT. The fuelling command was assumed to be available via a separate controller. Figure 2 shows the flow response for the reduced order model and Figure 3 shows the intake and exhaust manifold pressure profiles, the inset in Figure 3 depicts the pressure ratio trajectory, notice the satisfactory EGR flow regulation that is achieved as well as the smooth pressure ratio profile. The same controller was then implemented on the full order model; recall that the inputs to the full order model are the EGR valve position α and the VGT vane position β . Inverting the controller outputs, which are the respective flow rates, generated these inputs. Figure 4 shows satisfactory regulation of the desired flow rates though the EGR flow rate shows a non-monotonic behaviour. This is attributable to the direct influence of the manifold pressures on flow regulation for the full order model as was explained earlier.

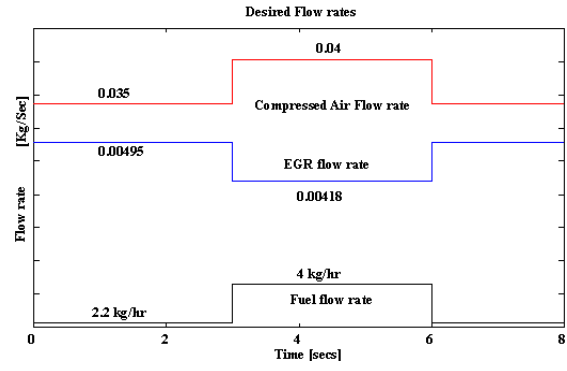


Figure 1: Reference values for regulation

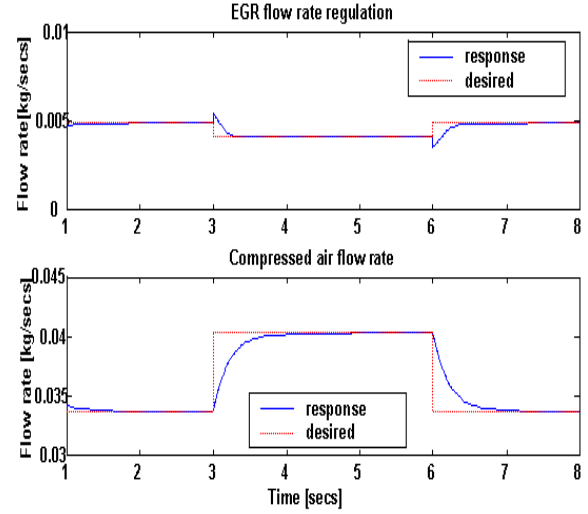


Figure 2: Reduced model response with MV SM control implementation

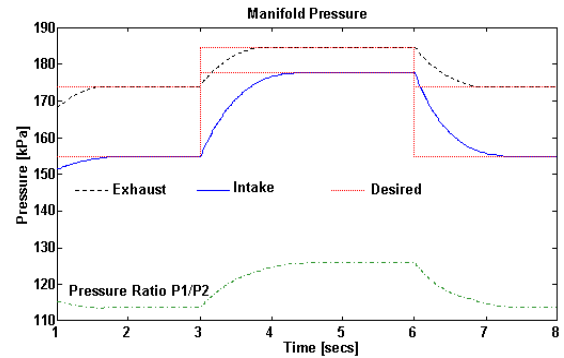


Figure 3: Manifold pressure response for the reduced model.

Figure 5 shows the manifold pressures along with the pressure ratio trajectory. Notice the correlation between the EGR flow response and the pressure ratio profile. Figure 6 shows the EGR valve and the VGT vane position response, while the vane behaves in a satisfactory manner the EGR valve response shows as much as 20% overshoot/undershoot. Again this is attributable to the model inversion approach that was used to estimate the EGR valve position and its sensitivity to the manifold pressure ratio.

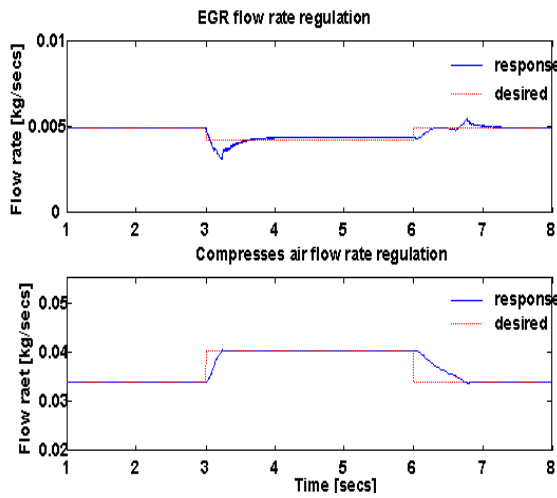


Figure 4: Response with MV SM control implementation on full order model

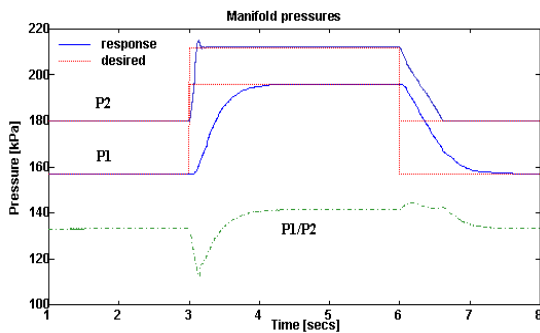


Figure 5: Manifold pressure response for full order model

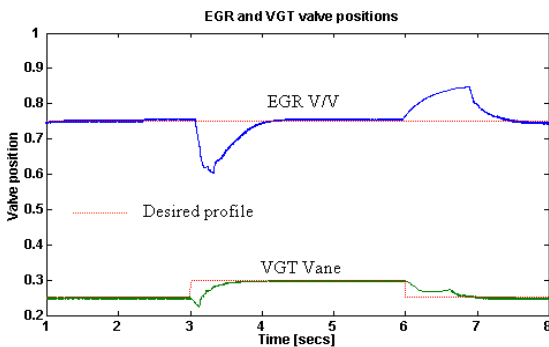


Figure 6: Valve position response for full order model

5. CONCLUSIONS

In this paper we presented the process for the design of a sliding mode controller for the coordinated control of VGT and EGR for a modern Diesel engine. The nonconformity of the plant model to the regular form design approach prompted us to extend the IO linearization technique to sliding mode control design. This allowed a systematic approach for the selection of the sliding surface as a simple extension of the IO linearization technique.

Simulation results showed the complex nature of the plant and the influence of the manifold pressures on the intake flow regulation process. It was noticed that the exact regulation of the EGR valve was the more difficult task. At this point we are unable to present experimental results from real time implementation of the proposed control algorithm. However, experimental verification of the controller performance will be taken up in the near future.

NOTATION

P_x = pressure; P_c = compressor power
 T_x = temperature; W_{xx} = mass flow rate
 C_p = sp. heat capacity; R_a = gas constant for air
 N = engine rpm; V = volume.

Greek letters and symbols

η = efficiency; τ = time constant;
 α = EGR valve position ; β = VGT vane position

Subscripts and Superscripts

1 = referenced to intake; 2 = referenced to exhaust

a = atmospheric; C1=from compressor to intake

2T = from exhaust manifold to turbine

TC = turbocharger; egr = exhaust gas recirculation

f = fuel; c = compressor; cis = isentropic for

compressor; tis = isentropic efficiency for turbine

tm = turbine mechanical; v = volumetric

D = displacement; d = desired value

REFERENCES

- Jankovich, M., M. Jankovich and I. Kolmanovsky (1998). Robust Nonlinear Control for Turbocharged Diesel Engines. *Proceedings of the American Control Conference*.
- Kolmanovsky, I., M. Van Nieuwstadt., P. Moraal and A. Stefanpoulou (1997). Issues in Modeling and Control of Intake Flow in Variable Geometry Turbocharged Engines. *Proceedings of the 18th IFIP Conference on System Modleing and Optimization*.
- Stefanapoulou, A., I. Kolmanovsky and J.S. Freudenberg (1998). Control of Vraiable Geometry Turbocharged Diesel Engines for Reduced Emissions. *Proceedings of the American Control Conference*.
- Slotine J.J and W. Li. *Applied Nonlinear Control* (1991). Prentice Hall, USA.
- Utkin, V., Hao-chi-Chang ., I. Kolmanovsky and J. Cook (2000). Sliding Mode Control for Variable Geometry Turbocharged Diesel Engines. *Proceedings of The American Control Conference*.
- Utkin, V (1991). *Sliding Modes in Control Optimization*. Springer Verlag U.S.A.
- Upadhyay, D (2001). *PhD Dissertation*. The Ohio-State University .
- Van Nieuwstadt, M., I. Kolmanovsky, and P. Moraal (2001). *Coordinated EGR-VGT Control for Diesel Engines: An Experimental Comparison..* SAE.